A Facile Route for the Preparation of Superparamagnetic Porous Carbons

Antonio B. Fuertes*,† and Pedro Tartaj*,‡

Instituto Nacional del Carbón (CSIC), Apartado 73, 33080 Oviedo, Spain, and Instituto de Ciencia de Materiales de Madrid (CSIC), Cantoblanco, 28049 Madrid, Spain

Received December 6, 2005. Revised Manuscript Received January 25, 2006

We present here a novel and simple synthetic strategy for fabricating superparamagnetic nanomagnets randomly dispersed in porous carbons. The method can be basically considered as a pyrolysis performed inside the restricted volume formed by the pores of an activated carbon. Such magnetic porous materials exhibit large surface areas (up to 1600 $m^2\ g^{-1}$), high pore volumes (up to 1.0 $cm^3\ g^{-1}$), and a porosity made up of accessible pores. An additional advantage of this method is its versatility, which allows composites with tunable magnetic properties to be obtained. In this way, it is possible to obtain superparamagnetic composites that can be easily manipulated by an external magnetic field.

Introduction

Materials that contain nanomagnets have shown great potential for use in advanced technological applications because of their exceptional properties.[1] Of special interest are those materials that exhibit superparamagnetic behavior at room temperature. In data storage applications, the particles must have a stable, switchable magnetic state to represent bits of information, a state that must not be affected by temperature fluctuations. However, for applications such as separation, the use of particles that present superparamagnetic behavior at room temperature (no remanence with a rapidly changing magnetic state) is preferred.[2] For example, nowadays, polymeric adsorbents containing superparamagnetic nanomagnets are used for the magnetic separation of biocompounds, and they have also proved to be a cost-effective way of removing transuranic elements from nuclear waste streams.[3]

To fully exploit the unique characteristics of materials containing superparamagnetic nanomagnets, it is necessary to develop new strategies that are able to add new functionalities to the resulting magnetic materials. In particular, the development of superparamagnetic composites of a large surface area and an accessible porosity would be a significant advance to improve or even extend the applicability of the magnetic separation technique in different fields (biomedicine, catalysis, waste treatment, etc.). To attain this objective, low-cost production strategies able to produce composites with tunable magnetic properties must be developed. In our opinion, a realistic strategy for the preparation of these composites should be based on the following principles: (a) the magnetic content should be provided by inexpensive, stable, and nontoxic materials such as iron oxides (magnetite or maghemite); (b) the magnetic properties of the resulting composites should be tunable in order to optimize the separation capacity by means of an electromagnet; (c) the matrix should be provided by a low-cost and widely available porous material. Commercial activated carbons (ACs) already widely used as adsorbents and catalytic supports, because of their low-cost, wide availability, and remarkable effectiveness, appear as good candidates for producing this kind of low-cost magnetic composite. ACs are often used in liquid media to remove contaminants, to recover valuable products, or to act as catalytic supports. Some examples of these applications include the removal of heavy metals and organic compounds in water, the extraction of gold complexes from gold leach solutions, and as supports of noble metal catalysts in hydrogenation processes.[4] In many of these cases, the separation of AC from the liquid medium is an essential step, which normally involves complex and expensive procedures such as filtration or centrifugation. The fabrication of magnetically separable activated carbons would greatly simplify the separation process, thereby making it more cost-effective.

* Author to whom correspondence should be addressed. Phone: +34-9-1334-9020. Fax: +34-9-1372-0623. E-mail: abefu@incar.csic.es (A.B.F.); ptartaj@icmm.csic.es (P.T.).

† Instituto Nacional del Carbón.

‡ Instituto de Ciencia de Materiales de Madrid.

(1) (a) Skumryev, V.; Stoyanov, S.; Zhang, Y.; Hadjipanayis, G.; Givord, D.; Nogués, J. *Nature* **2003**, *423*, 850. (b) Redl, F. X.; Cho, K.-S.; Murray, C. B.; O'Brien, S. O. *Nature* **2003**, *423*, 968. (c) Tartaj, P.; Serna, C. *J. Am. Chem. Soc.* **2003**, *125*, 15754. (d) Zhao, M.; Josephson, L.; Tang, Y.; Weissleder, R. *Angew. Chem., Int. Ed.* **2003**, *42*, 1375. (e) Li, Z.; Wei, L.; Gao, M.; Lei, H. *Adv. Mater.* **2005**, *17*, 1001. (f) Jeong, U.; Herricks, T.; Shahar, E.; Xia, Y. *J. Am. Chem. Soc.* **2005**, *127*, 1098. (g) Gupta, A. K.; Gupta, M. *Biomaterials* **2005**, *26*, 3995. (h) Berry, C. C. *J. Mater. Chem.* **2005**, *15*, 543.

(2) (a) Nam, J.-M.; Thaxton, C. S.; Mirkin, C. A. *Science* **2003**, *301*, 1884. (b) Pankhurst, Q. A.; Connolly, J.; Jones, S. K.; Dobson, J. *J. Phys. D: Appl. Phys.* **2003**, *36*, R167. (c) Tartaj, P.; Morales, M. P.; Veintemillas-Verdaguer, S.; Gonzalez-Carreño, T.; Serna, C. *J. Phys. D: Appl. Phys.* **2003**, *36*, R182. (d) Safarik, I.; Safarikova, M. *Biomagn. Reson. Technol.* **2004**, *2*, 7.

(3) Nuñez, L.; Kaminski, M. D. *J. Magn. Magn. Mater.* **1999**, *194*, 102.

(4) (a) Bansal, R. C.; Donnet, J.; Stoeckli, F. In *Active Carbon*; Marcel Dekker: New York, 1988; Chapter 6. (b) Radovic, L. R.; Rodriguez-Reinoso, F. Carbon Materials in Catalysis. In *Chemistry and Physics of Carbon*; Thrower, P. A., Ed.; Marcel Dekker: New York, 1997; Vol. 25, Chapter 3. (c) Radovic, L. R.; Moreno-Castilla, C.; Rivera-Utrilla, J. Carbon Materials as Adsorbents in Aqueous Solutions. In *Chemistry and Physics of Carbon*; Radovic, L. R., Ed.; Marcel Dekker: New York, 2001; Vol. 27, Chapter 4.

10.1021/cm052695e CCC: $33.50
Published on Web 02/24/2006

To our knowledge, the methods so far reported for the preparation of magnetic porous carbons do not satisfy all of the aforementioned requirements.[5] Thus, strategies based on high-energy milling techniques or the carbonization of an organic material (e.g., sawdust) impregnated with an iron salt are only able to retain a low portion of the porosity of the activated carbon.[5a,5b] Strategies based on the precipitation of iron oxides over active carbon particles led to the deposition of magnetic and nonmagnetic iron oxides made up of large aggregates (>100 nm).[5c] The method reported by Lu et al.,[5d] based on the deposition of metallic Co nanoparticles (11 nm) over the outer surface of an ordered carbon (CMK-3), has limitations due to the toxicity of cobalt and to the complex multistep synthetic route. Recently, Lee et al.[5e,5f] described a procedure for the preparation of magnetically separable mesoporous carbon (CMK-3) containing iron and iron oxide nanoparticles. This technique does not permit a control over the size of magnetic nanoparticles, and as a consequence, the resulting composite exhibits remanent magnetization, which limits its applicability.

We present here a novel, simple synthetic strategy for fabricating superparamagnetic porous carbons with tunable magnetic properties. The method consists of forming superparamagnetic nanoparticles of iron oxide ferrites, which are highly dispersed throughout the porous structure of a widely available commercial activated carbon. The preparation procedure involves, first, filling the porosity of the activated carbon with an appropriate amount of $Fe(NO_3)_3 \cdot 9H_2O$ dissolved in ethanol and, then, impregnating the dried sample with an organic reducing agent (ethylene glycol). Finally, the impregnated sample is treated under nitrogen at a moderate temperature in the 250−450 °C range. Our criterion for selecting the appropriate organic compound was based on the synthesis of nanoparticles, using polyols (ethylene glycol). Ethylene glycol is a reducing agent too weak to reduce Fe(II) ions to metallic iron (there was no interest on our part in preparing metallic iron nanoparticles because they are unstable against corrosion in a porous matrix), but it can reduce Fe(III) to give Fe(II) species essential for the formation of iron oxide ferrites.[6] Thus, the combination of the type of reducing agent, the temperature of pyrolysis, and the pore size of the carbon matrix may allow us not only to produce superparamagnetic iron oxide nanoparticles but also to control their size.

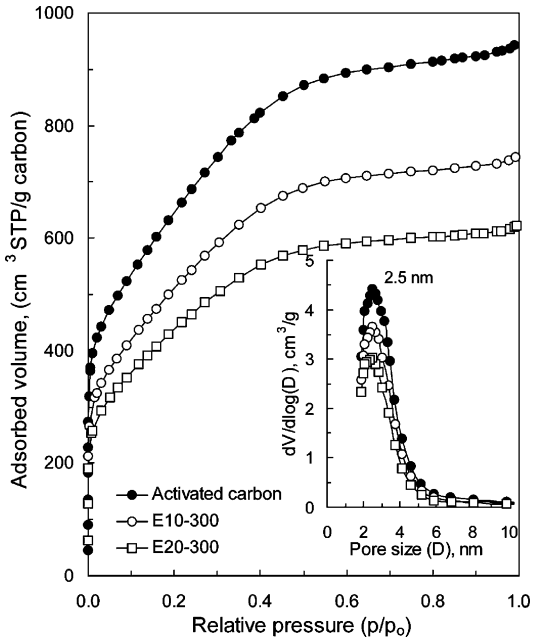

Figure 1. N_2 sorption isotherms and pore size distributions (inset) of the commercial activated carbon and samples containing 10% and 20% Fe.

Experimental Section

Starting Materials. A commercial activated carbon (M30) supplied by Osaka Gas (Japan) was used in these experiments. The commercial activated carbon used in this work exhibits a large Brunauer−Emmett−Teller (BET) surface area of 2350 $m^2\ g^{-1}$, a high pore volume of 1.47 $cm^3\ g^{-1}$, and a porosity made up of pores of up to 6−7 nm (distribution centered at around 2.5, see Figure 1, inset). Basically, our method can be considered as a pyrolysis performed inside the restricted volume formed by the pores of an activated carbon. Under these conditions, it can be expected that the growth of iron oxide nanoparticles will be partially limited by the size of the pores, a size that is in the range for superparamagnetic behavior at room temperature in iron oxide ferrites.[7] For the impregnation of activated carbon, $Fe(NO_3)_3 \cdot 9H_2O$ (Aldrich) was employed as the iron source. Ethylene glycol (Aldrich), which was used as a reducing agent, was purchased from Aldrich.

Fabrication of Magnetic Activated Carbon Materials. First, the porosity of the active carbon was filled with a solution of iron nitrate in ethanol. This was followed by drying at 90 °C for 2 h. In the preparation of the iron-impregnated active carbon samples, we added the precise volume of solution required to obtain a product with a 10 or 20 wt % Fe content. Once the iron salt was deposited inside the porosity of the activated carbon, the sample was impregnated with ethylene glycol up to incipient wetness (around 10 mmol of ethylene glycol per gram of carbon). The impregnated sample was then subjected to heat treatment under nitrogen at a temperature in the 250−450 °C range and maintained at this temperature for 2 h. The product obtained was cooled under nitrogen down to room temperature and was then exposed to a small stream of air in order to stabilize it. The materials obtained are denoted as *Ex − y*, *x* being the percentage of Fe and *y* the temperature of the thermal treatment in degrees Celsius. This study was restricted to samples with iron contents below 20 wt % and did not take into account higher concentrations because the porous composites can be readily manipulated by an external magnetic field (typically, a square magnet of 1 × 1 × 0.3 cm^3 with a B_r of 1 T) at these

(5) (a) Rudge, S. R.; Kurtz, T. L.; Vessely, C. R.; Catterall, L. G.; Williamson, D. L. *Biomaterials* **2000**, *21*, 1411. (b) Miller, J. D.; Munoz, G. A.; Duyvesteyn, S. Magnetic Activated Carbon Particles for Adsorption of Solutes from Solution. U.S. Patent Pub. No. US 2004/0147397 A1, July 29, 2004. (c) Oliveira, L.; Rios, R.; Fabris, J.; Garg, V.; Sapag, K.; Lago, R. *Carbon* **2002**, *40*, 2177. (d) Lu, A. H.; Schmidt, W.; Matoussevitch, N.; Bönnemann, H.; Spliethoff, B.; Tesche, B.; Bill, E.; Kiefer, W.; Schüth, F. *Angew. Chem., Int. Ed.* **2004**, *43*, 4303. (e) Lee, J.; Sunmi, J.; Hwang, Y.; Park, J. G.; Park, H. M.; Hyeon, T. *Carbon* **2005**, *43*, 2536. (f) Lee, J.; Lee, D.; Oh, E.; Kim, J.; Kim, H.-S.; Hwang, Y.; Kwan, J. H.; Park, J.-G.; Sin, C. H.; Kim, J.; Hyeon, T. *Angew. Chem., Int. Ed.* **2005**, *44*, 7427.

(6) (a) Viau, G.; Fievet, F. V.; Fievet, F. *J. Mater. Chem.* **1996**, *6*, 1047. (b) Cornell, R. M.; Schwertmann, U. In *The Iron Oxides. Structure, Properties, Reactions, Occurrence and Uses*; VCH: Weinheim, Germany, 1996. (c) da Costa, G. M.; Grave, E.; Bakker, P.; Vandenberghe, R. E. *J. Solid State Chem.* **1994**, *113*, 405.

(7) Morales, M. P.; Veintemillas, S.; Montero, M.; Serna, C.; Roig, A.; Casas, L.; Martinez, B.; Sandiumenge, F. *Chem. Mater.* **1999**, *11*, 3058.

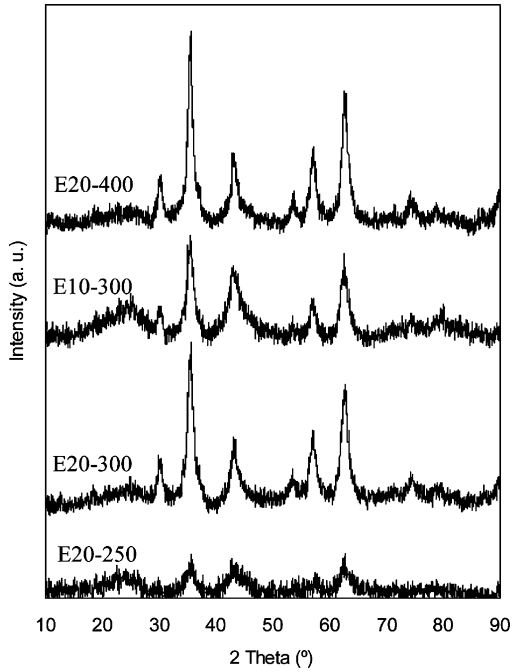

Figure 2. XRD patterns of samples showing only diffraction peaks associated with iron oxide with a spinel structure.

concentrations. Moreover, the addition of higher amounts of iron causes a notable reduction of the surface area available for the resulting composites.

Characterization. X-ray diffraction (XRD) patterns were obtained on a Siemens D5000 instrument operating at 40 kV and 20 mA, using Cu Kα radiation ($\lambda = 0.154\ 06$ nm). The cell parameters were determined by a least-squares fit of the data using silicon as a standard reference. The morphology of the powders was examined by transmission electron microscopy (TEM; 2000 FX2, JEOL). Nitrogen adsorption and desorption isotherms were performed at −196 °C in a Micromeritics ASAP 2010 volumetric adsorption system. The BET surface area was deduced by analyzing the isotherm in the relative pressure range of 0.04−0.20. The total pore volume was calculated from the amount of nitrogen adsorbed at a relative pressure of 0.99. The pore size distribution was calculated by means of the Kruk−Jaroniec−Sayari method.[8] The magnetic properties of the samples were recorded on a vibrating sample magnetometer (MLVSM9 MagLab 9 T, Oxford Instrument). The saturation magnetization (Ms) and coercivity field values (Hc) were obtained from the hysteresis loops registered up to a field of 5 T. Ms values were obtained from the law of approach to saturation.[9] The dependence of magnetization on temperature was monitored by zero-field-cooled (ZFC) experiments. The ZFC curve was obtained by first cooling the system in a zero magnetic field. The magnetic field was then applied (200 G), and the magnetization was measured as the temperature increased.

Results and Discussion

Evidence of the formation of iron oxide nanoparticles with a spinel structure (magnetite, Fe_3O_4, or maghemite, γ-Fe_2O_3) was obtained by XRD (Figure 2). A typical microstructure for composites with iron oxide spinel nanoparticles dispersed throughout the carbon matrix is displayed in Figure 3. Particle sizes obtained from the full width at half-maximum of the (311) and (440) iron oxide spinel reflections by using the Scherrer equation are all in the nanometric range (Table 1). The size of the nanoparticles deduced from the XRD measurements are in the range of the values estimated from the TEM images (see Figure 3). It is worth noting that the particle size distribution of the nanomagnets in the composites cannot be properly quantified from TEM because of poor contrast. Information about the distribution of magnetic nanoparticles in the porous matrix was obtained by chemical analyses carried out with an energy dispersive spectrometry in sections of different particles (Figure 4). This analysis

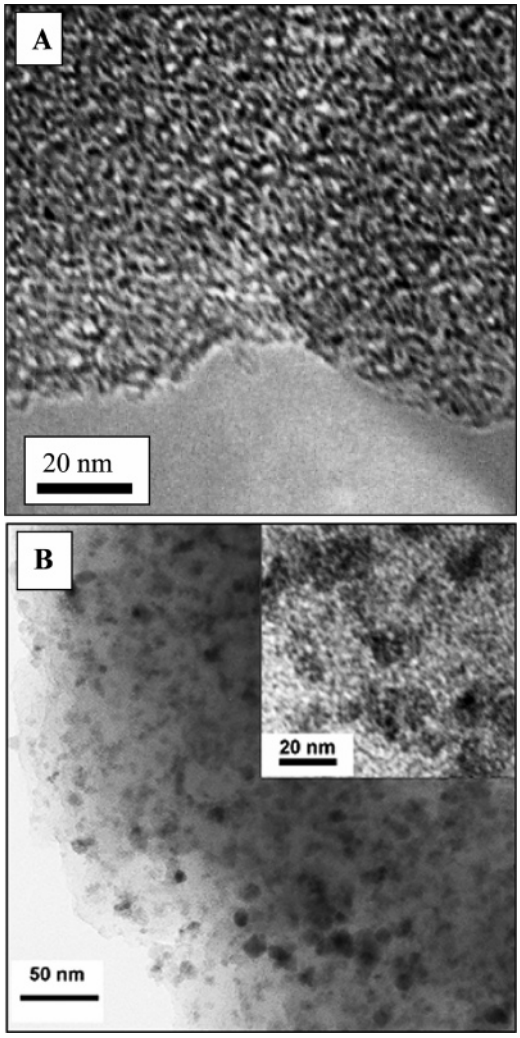

Figure 3. TEM images of (A) activated carbon and (B) the E20-400 composite showing the microstructure of samples (the dark spots correspond to areas containing nanomagnets). The inset is a magnification that shows that the porosity (bright spots) of active carbon is made up of disordered and fully interconnected pores.

Table 1. Summary of the Main Characteristics of Magnetic Porous Carbons[a]

sample	d_{XRD} (nm)	a (nm)[b]	S_{BET} ($m^2\ g^{-1}$)	Ms (emu g^{-1})	Hc (Oe)
E10-300	7	0.8380 (9)	1600	5.7	0
E20-250	4	0.8358 (9)	930	2.6	0
E20-300	7	0.8384 (7)	1130	11.8	0
E20-400	8	0.8381 (3)	1230	12.8	0

[a] The data included are the particle size (d_{XRD}) and cell parameter (a) values estimated by XRD. We also included the values of the BET surface area (S_{BET}) and the values of saturation magnetization (Ms) and the coercivity field (Hc) obtained at room temperature. [b] The standard deviation of the cell parameters is shown in parentheses.

(8) Kruk, M.; Jaroniec, M.; Sayari, A. *Langmuir* **1997**, *13*, 6267.
(9) Cullity, B. D. In *Introduction to Magnetic Materials*; Addison-Wesley: Reading, MA, 1972.

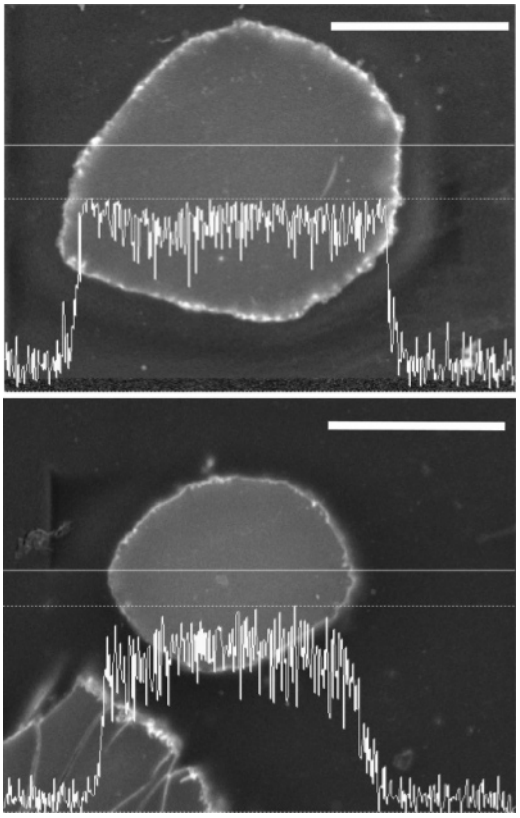

Figure 4. Iron distribution obtained by energy dispersive spectrometry in sections of two different particles (sample: E20-300). The noisy line represents the iron content. The continuous line represents the selected line for analysis, and the discontinuous line represents saturation of the signal (in our case, we are always below saturation, so the analysis is adequate). The iron content represented by the noisy line is constant in all of the profiles (from surface to center of the particle); that is, the iron oxide nanomagnets are equally distributed. (Bar length = 20 μm and scanning resolution $\sim$ 1 μm.)

shows a uniform distribution of Fe content from the surface to the center of the particle.

It seems surprising that nanoparticles of about 8 nm (i.e., E20-400) are obtained inside a porous network made up of pores below 6 nm (see Figure 1, inset). On the basis of the observations of the TEM images obtained for nonimpregnated (see Figure 3A) and impregnated (see inset in Figure 3B) samples, we believe that it is probably due to the fact that the porosity of carbon is made up of disordered and fully interconnected pores, which facilitates the growth of the iron oxide nanocrystals in all directions. Consequently, the size of the formed nanoparticles is not strictly limited by the nominal pore diameter of the activated carbon. A similar phenomenon has been observed in relation with the formation of large metal oxide nanostructures within the porosity of mesostructured silica materials with interconnected pores (i.e., SBA-15).[10] By contrast, when metal oxides are synthesized within the porosity of a material with noninterconnected pores (e.g., MCM-41), the growth of the nanoparticles is strictly limited by the size of the pores.[11] It should also be pointed out that the increase in particle size with temperature (Table 1) is in agreement with arguments based on the nucleation theory; that is, particle sizes increase with temperature.[12] Finally, it is important to emphasize that, in samples treated at 450 °C, the resulting iron oxide nanoparticles had similar sizes (8 nm) to those obtained at 400 °C. This suggests that the restricted volume formed by the pores of the activated carbon exert some restriction over the growing of the iron oxide nanoparticles.

Even though the difference between the magnetic moments of magnetite and maghemite are only about 15% in bulk, and for separation applications the use of either of these two phases or their solid solutions is equivalent, we accurately measured the cell parameters of the samples to discern the nature of the iron oxide present in the composites (Table 1). Magnetite has an inverse cubic spinel structure with oxygen forming a closely packed face-centered-cubic arrangement and Fe cations occupying interstitial tetrahedral and octahedral sites. Maghemite has a structure similar to that of magnetite and only differs in that all of the Fe is in the trivalent state. Cation vacancies compensate for the oxidation of Fe(II) cations. Logically, there exists a series of intermediate structures between magnetite and maghemite that differ in the number of their Fe(II) cations. Thus, even though both maghemite and magnetite have similar XRD patterns, their unit cell parameters are different (a = 0.834 nm for maghemite and 0.839 for magnetite).[6b] Consequently, if the cell parameters of the samples are measured accurately, it is possible to discern the nature of the iron oxide present in the composites. All of the samples (Table 1) have cell parameters between those of maghemite and magnetite, which suggests that the iron oxide phase present in the samples could be considered as a solid solution between magnetite and maghemite.[6b] In support of this assumption, sample E20-250 (having iron oxide of a smaller particle size and, thus, less stability against oxidation) has a cell parameter closer to maghemite, while the other samples have cell parameters closer to magnetite (Table 1). The fact that the cell parameters of all of the samples except E20-250 were similar suggests that magnetic nanoparticles above a certain size are stable against oxidation (this stability was confirmed by measuring the cell parameters of the samples 3 months after preparation, and it was found that the parameters were similar to those obtained immediately after the preparation of the samples).

The formation of iron oxide nanoparticles inside the porous structure of the active carbon causes a reduction of the porosity, which depends on the amount of iron oxide (see Figure 1) and the size of the nanoparticles. Thus, the BET surface area and pore volume values expressed on a carbon mass basis (normalized to carbon content) are, for E10-300, 1870 $m^2\ gC^{-1}$ and 1.15 $cm^3\ gC^{-1}$ and, for E20-300, 1580 $m^2\ gC^{-1}$ and 0.96 $cm^3\ gC^{-1}$, respectively. These results show that, although some of the pores of active carbon are blocked by the presence of nanoparticles, the composites still retain a large BET surface area and a high pore volume. It should also be noted that the BET surface area of the composites increases with the size of the nanoparticles (see samples E20-250, E20-300, and E20-400 in Table 1). This is probably

(10) Tian, B.; Liu, X.; Yang, H.; Xie, S.; Yu, C.; Tu, B.; Zhao, D. *Adv. Mater.* **2003**, *15*, 1370.
(11) Bourlinos, A.; Simopoulos, A.; Boukos, N.; Petridis, D. *J. Phys. Chem. B* **2001**, *105*, 7432.
(12) (a) Oxtoby, D. W. *Acc. Chem. Res.* **1998**, *31*, 91. (b) Ring, T. A. *Adv. Colloid Interface Sci.* **2001**, *91*, 473.

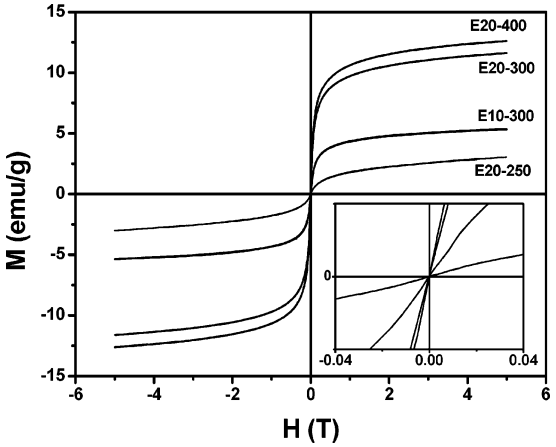

Figure 5. Magnetization curves of the samples. The inset shows a magnification of the low-field magnetization curve, in which the absence of remanence (zero coercivity) is clearly observed.

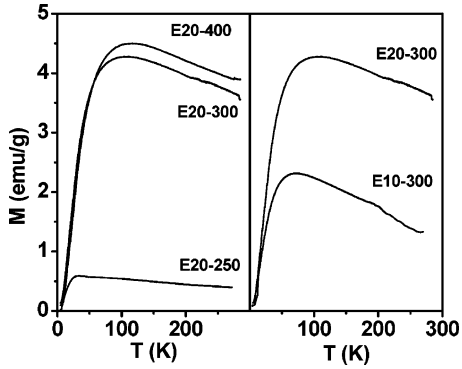

Figure 6. ZFC magnetization curves of samples as a function of temperature with an externally applied field of 200 Oe. The two curves illustrate the effect of particle size (E20-250, E20-300, and E20-400) and iron oxide concentration (E10-300 and E20-300), that is, an increase in the temperature at which the ZFC peak reaches its maximum as the particle size and iron oxide concentration increase.

because the smallest pores, which make a large contribution to the surface area, are preferentially blocked by the smallest nanoparticles.

Superparamagnetic behavior (i.e., zero coercivity field) at room temperature was detected in all of the samples (Table 1, Figure 5). The influence of the iron oxide particle size on the magnetic properties of the porous composites is reflected in the values of the saturation magnetization, which in ferrite nanoparticles are strongly dependent on particle size.[13] In particular, spin-canting phenomena produce a reduction of the saturation magnetization values, as the particle size decreases.[7] In our samples, this trend is clearly visible when samples of similar iron content and different ferrite particle size are compared (samples E20-250, E20-300, and E20-400 in Table 1). Here, it should be pointed out again that the difference between the magnetic moments of magnetite and maghemite are only about 15% in bulk. According to the XRD measurements, composites E10-300 and E20-300 contain iron oxide of similar particle size and crystallochemical characteristics. So, the Ms values normalized to the iron oxide content must be expected to be similar, as can be seen from Table 1 (sample E10-300 has about half the iron oxide content of sample E20-300, so its magnetization without being normalized to the iron oxide content will also show about half this value).

Similar results to those obtained from the Ms analysis were derived from the ZFC magnetization process (Figure 6). As expected, there is an increase in the temperature at which the ZFC peak reaches its maximum, T_M, with the increase in particle size (compare samples E20-250, E20-300, and E20-400 in Figure 6). More significant, however, is the shift to higher temperatures of T_M when the iron oxide concentration in samples of a similar particle size and crystallochemical characteristics is increased (compare samples E10-300 and E20-300 in Figure 6). Interparticle dipolar interactions also affect the effective anisotropy energy and change the temperature at which a particle becomes superparamagnetic.[14] Normally, there is a shift of the maximum temperature to a higher temperature as a result of an increase in the relaxation times.[14b] Thus, the magnetic properties of these composites must be the result of competition between the intrinsic anisotropy energy and interparticle dipolar interactions. It is also worth noting that the smoothness of the peaks in all of the samples could reflect some broad particle size distribution of the nanomagnets, though dipolar interactions between nanomagnets and their possible intrinsic disorder could also be the basis for the observed smoothness.

Conclusions

We have illustrated a procedure for successfully fabricating superparamagnetic porous carbons through the synthesis of iron oxide magnetic nanoparticles inside the pores of a commercial activated carbon. This method suggests a simple route for the synthesis of magnetically separable active carbons. Such magnetic porous materials exhibit large surface areas (up to 1600 $m^2\ g^{-1}$), high pore volumes (up to 1.0 $cm^3\ g^{-1}$), and a porosity made up of accessible pores. An additional advantage of this method is its versatility, which allows the obtainment of superparamagnetic composites that can be easily manipulated by an external magnetic field (typically, a square magnet of $1 \times 1 \times 0.3$ cm^3 with a B_r of 1 T). Furthermore, because it is possible to functionalize the carbon surface by inserting a polymeric phase inside the porous network of the composite,[15] these materials could be used for advanced applications in areas such as the selective separation of biomolecules or the fabrication of high-performance catalysts.

Acknowledgment. The financial support for this research provided by the MEC (MAT2005-00262, MAT2005-03179, and NANO2004-08805-C04-01) is gratefully acknowledged.

CM052695E

(13) (a) Martinez, B.; Obradors, X.; Balcells, L.; Rouanet, A.; Monty, C. *Phys. Rev. Lett.* **1998**, *80*, 181. (b) Tartaj, P.; González-Carreño, T.; Serna, C. *Adv. Mater.* **2001**, *13*, 1620. (c) Tartaj, P.; González-Carreño, T.; Serna, C. *Adv. Mater.* **2004**, *16*, 529. (d) Lee, Y.; Lee, J.; Bae, C. J.; Park, J.-G.; Noh, H.-J.; Park, J.-H.; Hyeon, T. *Adv. Funct. Mater.* **2005**, *15*, 503.

(14) (a) El-Hilo, M.; O'Grady, K.; Chantrell, R. W. *J. Magn. Magn. Mater.* **1992**, *114*, 295. (b) Mørup, S.; Bødker, F.; Hendriksen, P. V.; Linderoth, S. *Phys. Rev. B* **1995**, *52*, 287.

(15) (a) Choi, M.; Ryoo, R. *Nat. Mater.* **2003**, *2*, 473. (b) Choi, M.; Kleitz, F.; Liu, D.; Lee, H.-Y.; Ahn, W.-S.; Ryoo, R. *J. Am. Chem. Soc.* **2005**, *127*, 1924.